2nd International Conference on Current Research Trends in Engineering and Technology
© 2018 IJSRSET | Volume 4 | Issue 5 | Print ISSN: 2395-1990 | Online ISSN : 2394-4099
Themed Section: Engineering and Technology

A Review on CFD Analysis of Porous Ceramic Hydrodynamic Journal Bearing

Baria Divyesh[1], Jaganiya Mayank[2], Saurabh Singh[3],
Mr. Sorathiya Mehul[4]
[1-3]U.G. Student, Mechanical Engineering, Sigma Institute of Engineering, Vadodara, Gujarat, India
[4]Assistant Professor, Mechanical Engineering, Sigma Institute of Engineering, Vadodara, Gujarat, India

ABSTRACT

This paper relates to a review on cfd analysis of journal bearing for brass and silicon nitride material. This review is focused on finding velocity and pressure distribution of the journal bearing for brass and silicon nitride material. We are going to increase the bearing life and capacity. The CFD analysis in the velocity and pressure difference comparing for brass and silicon nitride material journal bearing. hydrostatic journal bearing is a bearing operating with hydrodynamic lubrication by virtue of their overall performance porous ceramic hydrodynamic journal bearing present themselves as a viable solution to the newest severs demand for higher accuracy and overall performance levels required by spindle bearing systems.

Keywords: cfd analysis, journal bearing, hydrodynamic.

I. INTRODUCTION

In India water cooled type submersible motors are extensively manufactured and available in the market due to its simplicity in design and manufacture. The maintenance of such motors is also very simple and can be carried out t ease compared to the oil filled version.

Even with such advantages water cooled submersible motors too pose various problems especially with its bearing.

Figure 1.0 worm out bearing bush

The bearing bush is brass material , we are selecting the silicon nitride material for bush bearing, and analysis of the silicon nitride material bearing.

Figure 1.1 Worm out bearing surface of the rotor

II. Problem Identification

This was a long standing problem at M/s vira pumps, Kolhapur, Maharashtra, India for around 5 years. This industry is a reputed manufacture and exporter of submersible pumps. It has started producing 100 mm (4”) submersible motors since 2001.figure 1.2 shows a sectional view of such a submersible motor.

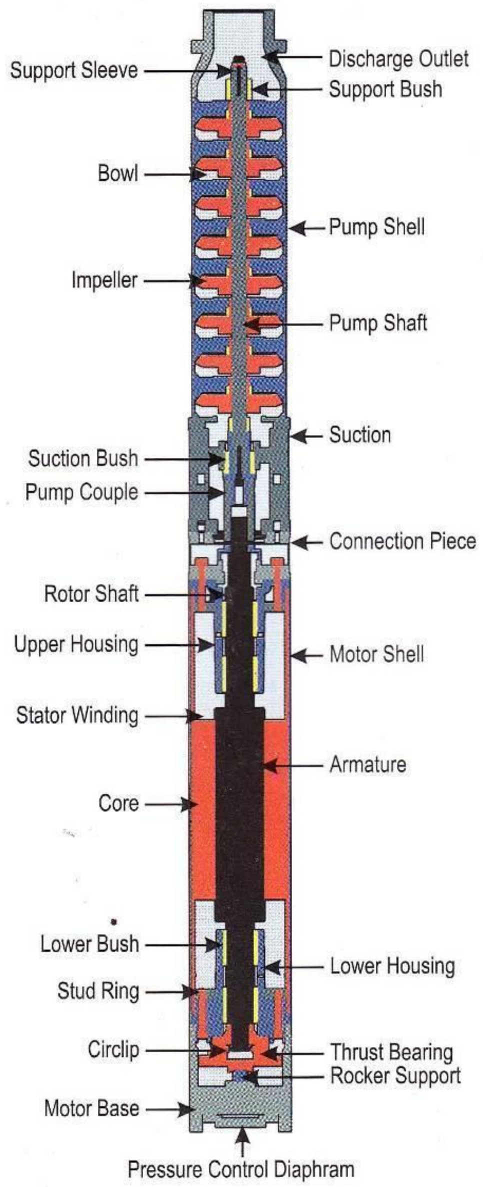

For motors above 1.0 hp, it experienced bearing bush failure after just few months of operation. Where as its earlier products i.e. 150 mm and 200 mm submersible motors operated smoothly for more than 25 years. Due to this industry faced huge problems in their operations. They were not only the ones who suffered but, similar manufactures in India experienced the same problem.

This problem solving we are selecting the material for bush bearing is silicon nitride. It has a frictionless, high heat absorption, capacity, light weight.

The root cause analysis suggest that the following factors are responsible for such bearing bush failures:

1. Velocity changes
2. Pressure distributions
3. Fatigue analysis/life of bush
4. FEA structural analysis

The cfd analysis in the results is almost same in velocity changes for brass and silicon nitride material bush bearing. The pressure distribution is low in silicon nitride material bush bearings and high in the brass material bush bearings.

III. LITERATURE

This was a long standing problem at M/s vira pumps, Kolhapur, Maharashtra, India for around 5 years. This industry is a reputed manufacture and exporter of submersible pumps. It has started producing 100 mm (4”) submersible motors since 2001.figure 1.2 shows a sectional view of such a submersible motor. For motors above 1.0 hp, it experienced bearing bush failure after just few months of operation. Where as its earlier products i.e. 150 mm and 200 mm submersible motors operated smoothly for more than 25 years. Due to this industry faced huge problems in their operations. They were not only the ones who suffered but, similar manufactures in India experienced the same problem.

B. Manshoor, M. Jaat, Zaman Izzuddin, Khalid Amir (2013); In this, there was a introduction about cfd analysis of thin film lubricated journal bearing. In this paper, three turbulent models which are the standard k-e model and Reynolds stress model had been used to simulate the characteristics of a plain journal bearing.

Therefore, in this case study it was revealed that, the k-e model was just enough to do the simulation since it was the simplest model compared to other.

Ravindra M. Patel (2013):- This paper studies the 3D model of hydrodynamic plain journal bearing using COMSOL software. Generalized Reynolds equation is used for analysing hydrodynamic journal bearing by COMSOL as well as by analytical method by applying Somerfield boundary conditions. The pressure distribution of the hydrodynamic plain journal bearing lubricated with oil under steady state consideration has been analysed.

Miss. Kirtee L. Chidle, Dr. Mrs. R.N. Baxi (2016):- This paper presents a review of the performance analysis of journal bearing. Major emphasis is given to the pressure and temperature distribution based identification analysis on bearing. This paper attempts to evaluate the journal bearing performance on various parameters such as pressure distribution, bearing surface deformation, temperature distribution and load carrying capacity.

Dinesh Dhande, Dr. D. W. Pande, Vikas Chatarkar (2013):- In this paper, journal bearing models are developed for different speeds and eccentricity ratios to study the interaction between the fluid and elastic behaviour of the bearing. The nodal fluid forces computed by CFD are used in order to find deflection of the bearing. Cavitations in the bearing are neglecting by setting all negative pressure to ambient pressures. The bearing wall is considered as stationary and journal is modelled as moving wall. The sides of the lubricant volume have been assigned with a zero pressure condition, meaning that the lubricant is free to flow rate.

Amit Chauhan (2016):- In this paper, The model has been simulated using the ANSYS Fluent Software which solves 3-Dimensional Navier Stokes and Energy equation for finding the thermal performance characteristics of the bearing. The lubricant flow has been considered as laminar. The distribution of pressure and temperature throughout the bearing has been obtained by Iso-thermal approach and by thermo-hydrodynamic approach. Thermo-hydrodynamic analysis for circular journal bearing has been carried out using the application of Computational Fluid Dynamics.

P Hanoca, H. V. Ramakrishna (2015):- In this paper the oil film thickness between slider and shoe is a significant parameter and has a strong influence on the bearings performance. A CFD analysis has been carried out to find the effect of oil film thickness at the entrance of the slider using ANSYS workbench. Laminar viscous model with SIMPLE pressure-velocity coupling are used for the analysis. 2-D steady state, Navier-Stoke equations are discretized with finite volume approximations using structured grids. Pressure distribution over the slider and load carrying capacity increases up to some extent later decreases. Viscosity plays a very vital role in load carrying capacity. As the viscosity drops, the load carrying capacity also decreases.

IV. RESULTS

CFD Analysis Of bush bearings

The conventional method in designing a journal bearing is by using a bearing pressure recommended for specific applications. In the case of submersible motor it is recommended to use a bearing pressure in the range 0.7 to 1.4 as shown in table 1.0

Machinery	Bearing	l/d	Permissible bearing Pressure (N/mm^2)
Gas And oil	Main	0.6-2.0	4.9-8.4

Engines (4-stroke)	Crank pin Wrist pin	0.6-1.5 1.5-2.0	10.8-12.6 12.5-15.4
Gas and oil engines (2-stroke)	Main Crank pin Wrist pin	0.8-1.8 0.7-1.4 1.5-2.2	5.6-11.9 10.5-24.5 16.1-35.0

Aircraft And Automobile engines	Main Crank pin Wrist pin	0.8-1.8 0.7-1.4 1.5-2.2	5.6-11.9 10.5-24.5 16.1-35.0
Reciprocating Compressors and pumps	Main Crank pin Wrist pin	1.0-2.2 0.9-1.7 1.5-2.0	1.75 4.2 7.0
Centrifugal pumps, motors And generators	Rotor	1.0-2.0	0.7-2.0
Railway cars	Axle	1.9	3.5
Marine steam engines	Main Crank pin Wrist pin	0.7-1.5 0.7-1.2 1.2-1.7	3.5 4.2 10.5
Punching And shearing machines	Main Crank pin	1.0-2.0 1.0-2.0	28 56
Rolling Mills	Main	1.0-1.5	21

Table 1.0 permissible bearing pressure

Instead of taking the value directly from the above table, we will perform CFD analysis on the bearing; by this we will also be able to verify the value of bearing pressure 'p'. We can use then the value obtained from the analysis and perform the design step to calculate the length of bush bearing.

Figure shows the CFD analysis, ansys software is used for the CFD analysis .The journal in this case is rotated at 1800 rpm which is rated speed of motor. The working fluid is chosen as water.

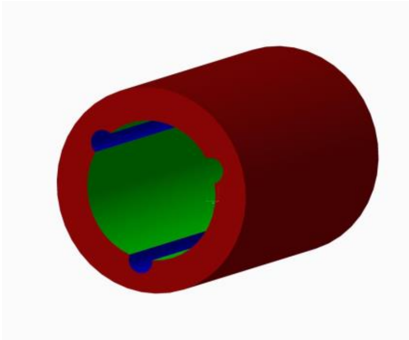

FIGURE II.I. CAD Model in Creo

Dimensions of the Journal
Outer dia. 23 mm
Inner dia. 19 mm
Length 40 mm

IV.I. CFD Analysis for brass material journal bearing

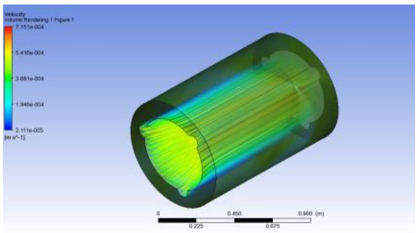

Figure 3.1.1 ISO VIEW

Figure 3.1.1 describe Iso-metric image after simulate the model with the help of input data we can see the contour line present in the bush which is made by Velocity contours. In addition, material applied to the model so, it represents the BRASS textures.

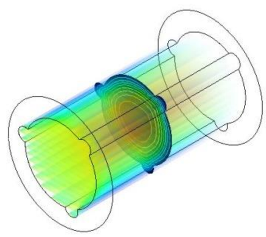

Figure 3.1.2 VELOCITY CONTOUR AT CENTRE

Figure 3.1.2 describe Iso-metric image after simulate the model with the help of input data we can see the sectioned contour over the section plane present in the bush which is made by Velocity contours. Outer material made transparent, so, inside section contour can be visible. Section plane contour is located at particular location in the model.

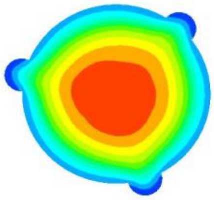

Figure 3.1.3 VELOCITY PROFILE AT CENTRE

Figure 3.1.3 describe left hand side view image after simulate the model with the help of input data we can see the sectioned contour over the section plane present in the bush which is made by Velocity contours. We can see that at the boundary of bush the velocity is low as compared to centre of the bush. Which represent the frictional effect of the wall boundary. Section plane contour is located at particular location in the model.

Inlet 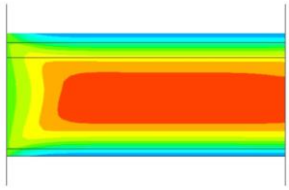 Outlet

Figure 3.1.4 VELOCITY PROFILE SECTION VIEW

Figure 3.1.4 describe top view side view image after simulate the model with the help of input data we can see the sectioned contour over the section plane present in the bush which is made by Velocity contours. We can see that at the boundary of bush the velocity is low as compared to centre of the brass material bush. Which represent the frictional effect of the wall boundary. Section plane contour is located at particular location in the model.

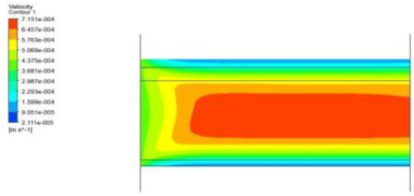

Figure 3.1.5 VELOCITY PROFILE

Figure 3.1.5 describe top view side view image after simulate the model with the help of input data we can see the sectioned contour over the section plane present in the bush which is made by Velocity contours. We can see that at the boundary of bush the velocity is low as compared to centre of the bush. Which represent the frictional effect of the wall boundary. Section plane contour is located at particular location in the model. The graph shown at the left side of the image represents minimum and maximum value of the velocity.

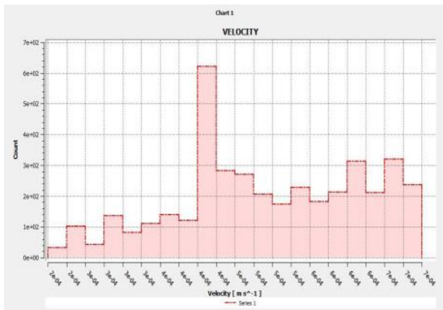

3.1.6 Velocity Graph of Brass Material Journal Bearing

Velocity vs chart count graph shows the velocity of fluid flows from inlet to outlet in which velocity is higher at centre portion and low at nearer to wall area.

Figure 3.1.7 Pressure Distribution Graph for Brass

Pressure vs chart count graph shows the pressure distribution of fluid from inlet to outlet in which pressure is higher at inlet side of the component and lower at the outlet side.

IV.II. CFD Analysis for silicon nitride material Journal bearing

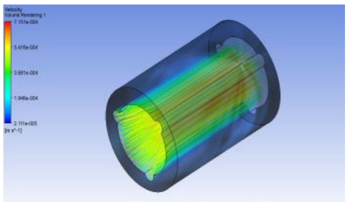

Figure ISO VIEW

Figure 3.2.1 describe Iso-metric image after simulate the model with the help of input data we can see the contour line present in the bush which is made by Velocity contours. In addition, material applied to the model so, it represents the SILICON-NITRIDE textures.

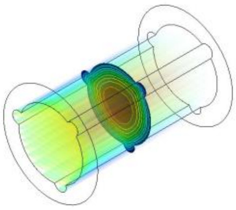

Figure 3.2.2 VELOCITY CONTOUR AT CENTRE

Figure 3.2.1 describe Iso-metric image after simulate the model with the help of input data we can see the sectioned contour over the section plane present in the bush which is made by Velocity contours. Outer material made transparent, so, inside section contour can be visible. Section plane contour is located at particular location in the model.

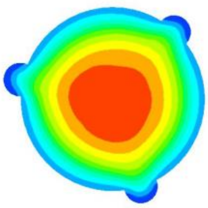

Figure 3.2.3 VELOCITY PROFILE AT CENTRE

Figure 3.2.3 describe left hand side view image after simulate the model with the help of input data we can see the sectioned contour over the section plane present in the bush which is made by Velocity contours. We can see that at the boundary of bush the velocity is low as compared to centre of the bush. Which represent the frictional effect of the wall boundary. Section plane contour is located at particular location in the model.

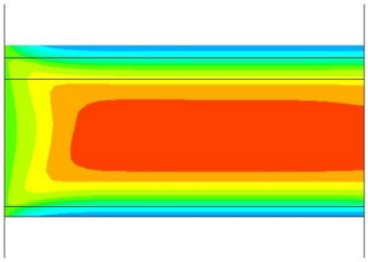

Figure 3.2.4 VELOCITY PROFILE SECTION VIEW

Figure 3.2.4 describe top view side view image after simulate the model with the help of input data we can see the sectioned contour over the section plane present in the bush which is made by Velocity contours. We can see that at the boundary of bush the velocity is low as compared to centre of the silicon nitride material bush.Which represent the frictional effect of the wall boundary. Section plane contour is located at particular location in the model.

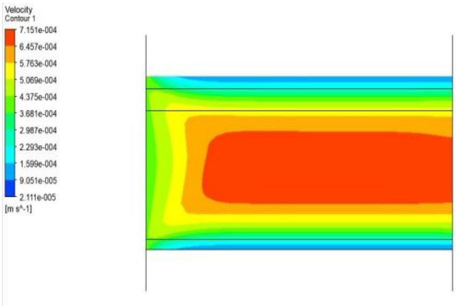

Figure 3.2.5 VELOCITY PROFILE

Figure 3.2.5 describe top view side view image after simulate the model with the help of input data we can see the sectioned contour over the section plane present in the bush which is made by Velocity contours. We can see that at the boundary of bush the velocity is low as compared to centre of the bush. Which represent the frictional effect of the wall boundary. Section plane contour is located at particular location in the model. The graph shown at the left side of the image represents minimum and maximum value of the velocity.

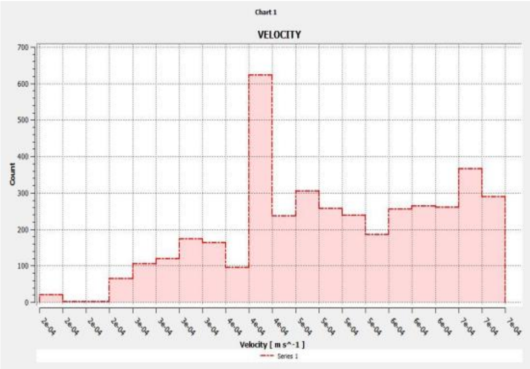

Figure 3.2.6 Velocity Graph of Brass Material Journal Bearing

Velocity vs chart count graph shows the velocity of fluid flows from inlet to outlet in which velocity is higher at centre portion and low at nearer to wall area.

Figure 3.2.7 Pressure Distribution Graph for Brass

Pressure vs chart count graph shows the pressure distribution of fluid from inlet to outlet in which pressure is higher at inlet side of the component and lower at the outlet side.

V. CONCLUSION

With the help of CFD analysis on both materials,
We can conclude that,
Uses of different material Brass and Silicon Nitride

1. There is not any difference in fluid flow pattern.
2. There is not any difference in contour.
3. Velocity profiles are remaining same for both materials.

Therefore, Velocity flow profile remains the same for all type of materials.

VI. Future scope

Working on process Structural load carrying capacity, Working on process Bearing life / Fatigue analysis, Manufacture ceramic bearing, testing the new bearing in comparison to steel bearing.

VII. REFERENCES

[1] B. Manshoor, M. Jaat, Zaman Izzuddin, Khalid Amir (2013); “CFD Analysis of Thin Film Lubricated Journal Bearing” The Malaysian International Tribology Conference, Energy and Industrial Environment Studies (CEIES), University Johor, Malaysia.

[2] Ravindra M. (2013 Analysis of Hydrodynamic Plain Journal Bearing Sardar Vallabhbhai National Institute of Technology, Surat, Gujarat, India.

[3] Miss. Kirtee L. Chidle, Dr. Mrs. R.N. Baxi (2016); “CFD ANALYSIS OF FLUID FILM JOURNAL BEARING: A REVIEW” International Research Journal of Engineering and Technology, G. H. Raisoni college of Engineering, Nagpur, Maharashtra, India.

[4] Dinesh Dhande, Dr. D. W. Pande, Vikas Chatarkar (2013) “Analysis of Hydrodynamic Journal Bearing using fluid structure interaction” International journal of engineering trends and technology, AISSMS Collage of engineering, Pune.

[5] Amit Chauhan (July 2014); “Circular Bearing Performance Parameters with Isothermal And Thermo-Hydrodynamic Approach Using Computational Dynamics” International Journal of Research in Advent Technology, university institute of engineering and technology, Punjab university, Chandigarh, India.

[6] P Hanoca, H. V. Ramakrishna (2015); “To Investigation the Effect of Oil Thickness at the Entrance of the Infinitely Long Slider

Bearing Using CFD Analysis" International conference on computational heat and mass transfer, maland collage of engineering Hassan, India.

[7] Srinivasan V. School of Mechanical Engineering, Bharath University, Chennai, (INDIA) "Analysis of static and dynamic load on hydrostatic bearing with variable viscosity affected by the environmental temperature" J. Environ. Research Develop.Vol. 7 No. 1A, July-September 2012.

[8] K.J. Metman, E.A. Muijderman, G.J.J. van Heijningen, and D.M. Halemane "Load carrying capacity of multi-recess hydrostatic journal bearing at high eccentricities" department mechanical engineering, Tribology international journal, Butterworth & co (publisher) ltd, vol. 19 , 1986.

[9] Lozysko slizgowe, przeplyw oleju, metoda elementow, skonczonych "The flow oil analysis in the gap of a journal bearing with a circumferential groove" Faculty of Mechanical Engineering and Aeronautics, Rzeszow University of Technology, Al. Powstancow Warszawa Rzeszow, Poland 2009.

[10] D. M. Nuruzzaman, M. K. Khalil, M. A. Chowdhury, M. L. Rahaman "Gazipur "Study on pressure distribution and load capacity of a journal bearing using finite element method and analytical method" Department of Mechanical Engineering Dhaka University of Engineering & Technology, Gazipur, International Journal of Mechanical & Mechatronics Engineering IJMME-IJENS 2010.